

LOCALIZED BURSTY PLASMA FLOW IN THE NIGHTSIDE
IONOSPHERE—IMPLICATION FOR DISTANT TAIL
RECONNECTION (EXTENDED ABSTRACT)

Masakazu WATANABE¹, Michael PINNOCK², Alan S. RODGER², Natsuo SATO¹,
Hisao YAMAGISHI¹, A. Sessai YUKIMATU¹, Raymond A. GREENWALD³,
Jean-Paul VILLAIN⁴ and Marc R. HAIRSTON⁵

¹*National Institute of Polar Research, 9–10, Kaga 1-chome, Itabashi-ku,
Tokyo 173-8515*

²*British Antarctic Survey, Natural Environment Research Council, High Cross,
Madingley Road, Cambridge CB3 0ET, U. K.*

³*Applied Physics Laboratory, The Johns Hopkins University, Johns Hopkins Road,
Laurel, Maryland 20723-6099, U. S. A.*

⁴*Laboratoire de Physique et Chimie de l'Environnement, Centre National de la
Recherche Scientifique, 3A Avenue de la Recherche Scientifique, 45071 Orléans,
Cedex 2, France*

⁵*William B. Hanson Center for Space Sciences, University of Texas at Dallas,
P.O. Box 830688 F022, Richardson, Texas 75083-0688, U. S. A.*

Magnetic reconnection is one of the major paradigms of magnetospheric physics, at least in phenomenology. To date, ionospheric signatures of reconnection have been reported by many authors; however, almost all of these reports are on dayside reconnection. In this paper, we report on two equatorward bursty plasma flow events (one on November 16, 1995 and the other on October 27, 1995) observed by Goose Bay-Stokkseyri dual HF radars in the nightside ionosphere that would be relevant to distant tail reconnection. Both occurred during a late substorm growth phase just prior to the expansion phase onset. In this article we will briefly describe one of the two events.

The event we demonstrate here occurred on November 16, 1995. Figure 1 shows the horizontal component (positive geomagnetic north) of the ground magnetic field observed at Thule (THL, near geomagnetic north pole), Fort Churchill (FCC, auroral zone in the evening sector), Ottawa (OTT, mid-latitude in the evening sector), Narssarssuaq (NAQ, premidnight auroral zone), and Tromsø (TRO, midnight auroral zone). At 2219 UT (the vertical broken line on the left), an eastward electrojet started to enhance in the evening sector as indicated by positive excursions at Fort Churchill and Ottawa; at this time positive magnetic field deflections were also observed at Thule and Narssarssuaq. These suggest that a substorm growth phase started at 2219. At 2327 UT, a sharp negative bay started at Tromsø as denoted by the vertical broken line on the right, which is the onset of the substorm expansion phase. Thus, a substorm followed after a long period of a quiet magnetosphere associated with a northward interplanetary magnetic field (not shown here). The time interval bounded by the two vertical broken lines is the growth phase of the substorm. The bursty plasma flow

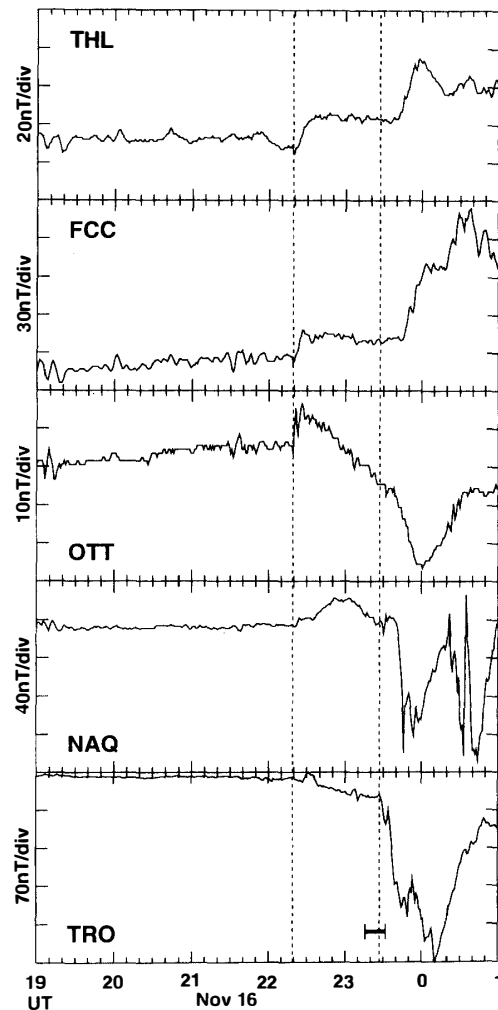


Fig. 1. The horizontal component (positive geomagnetic north) of the ground magnetic field on November 16, 1995, observed at Thule (THL, near geomagnetic north pole), Fort Churchill (FCC, auroral zone in the evening sector), Ottawa (OTT, mid-latitude in the evening sector), Narsarsuaq (NAQ, premidnight auroral zone), and Tromsø (TRO, midnight auroral zone). The vertical broken lines show the start of the substorm growth phase (2219) and the onset of the expansion phase at Tromsø (2327). The bursty plasma flow occurred during the interval indicated by the horizontal bar in the bottom Tromsø magnetogram.

we describe here occurred from 2316 to 2332 as denoted by the horizontal bar in the bottom panel of Fig. 1 (Tromsø magnetogram), most of which corresponded to the late growth phase just prior to the expansion phase onset.

In this paper we have analyzed data from a Goose Bay (Canada)-Stokkseyri (Iceland) HF radar pair. These radars are part of Super Dual Auroral Radar Network (SuperDARN) and observe a large volume of the ionosphere above northeastern Canada and Greenland. They operate at frequencies between 8 and 20 MHz and measure the coherent backscattered power and Doppler spectral characteristics of field-aligned irregularities in the *E* and *F* regions (see GREENWALD *et al.*, 1995 and refer-

ences therein for detailed description). At F -region altitudes, the line-of-sight Doppler velocity gives a reasonable measure of the electric field drift of plasmas. In usual operation mode, all the SuperDARN radars scan over an azimuthal sector in 16 beam steps every two minutes, and the backscatter returns are range-gated in steps of 45 km. The radars are located in pairs in order to measure a common volume by two radars. In the common viewing area of each radar pair, a two-dimensional map of plasma convection is produced every two minutes by composing the line-of-sight Doppler velocities from both radars. During the time intervals of the two events analyzed here, the radars were operated in this usual operation mode. In this paper, we will present the characteristics of the bursty flow of plasmas using exclusively Goose Bay data, although we have also analyzed the data from Stokkseyri radar, the other radar of the pair. Goose Bay radar is located at 53.3°N , 60.5°W in geographic coordinates and it scans over a 52° azimuth sector centered on 5° east of geographic north. In the forthcoming Fig. 2, examples of backscatter echoes of the Goose Bay radar are shown in the AACGM (altitude adjusted corrected geomagnetic) coordinate system based on the International Geomagnetic Reference Field Epoch 1995. In this paper we assumed that the F region echoes are scattered at 400 km altitude. For a practical algorithm for computing the AACGM coordinate system, see BHAVNANI and HEIN (1994).

Figure 2 shows a time sequence of Doppler velocities for each two-minute scan from 2310 to 2334 observed by the Goose Bay radar. Cold colors represent velocities toward the radar, whereas warm colors show velocities away from the radar. In panel e (2318–20), we can see a localized light-blue region of equatorward bursty flow in the middle of field-of-view (denoted by a yellowish green arrow). Doppler velocities of this region are greater than 750 m/s towards the radar. This flow burst is the subject of our present study. In the next scan (panel f, 2320–22), the bursty flow is also discernible as a light-blue (>750 m/s) region, but its location migrated a little equatorward as compared with the previous scan. In the next two scans (panels g and h, 2322–26), the bursty flow region continues to exist well isolated by its surrounding regions and its location migrates further equatorward with time. At the next scan (panel i, 2326–28), when the expansion phase onset occurred, the major bursty flow has almost disappeared, although a light-blue high flow speed region can be identified as indicated by a yellowish green arrow. This high flow speed region can be traced in the next two scans (panels j and k, 2328–32), but it finally dies away at ≈ 2332 (panel l, 2332–34). On the other hand, to return to the start of the bursty flow, the equatorward migrating flow burst can be traceable from the scan of panel d (2316–18), although its main part is somewhat contaminated by noise. However, we cannot trace the bursty flow prior to that scan; in the preceding three scans (panels a through c, 2310–16), we cannot discern a significant high flow speed region. To sum up, an equatorward bursty flow region with velocities greater than 750 m/s emerged abruptly at ≈ 2316 (panel d) and migrated equatorward with time; it started to degenerate at the substorm expansion phase onset (≈ 2326 , panel i) and finally faded out at ≈ 2332 (panel l).

Plasma velocities shown in Fig. 2 are only the line-of-sight component observed by the Goose Bay radar. The Stokkseyri radar, which is located to the east of the Goose Bay radar, was also operational and we could construct two-dimensional maps

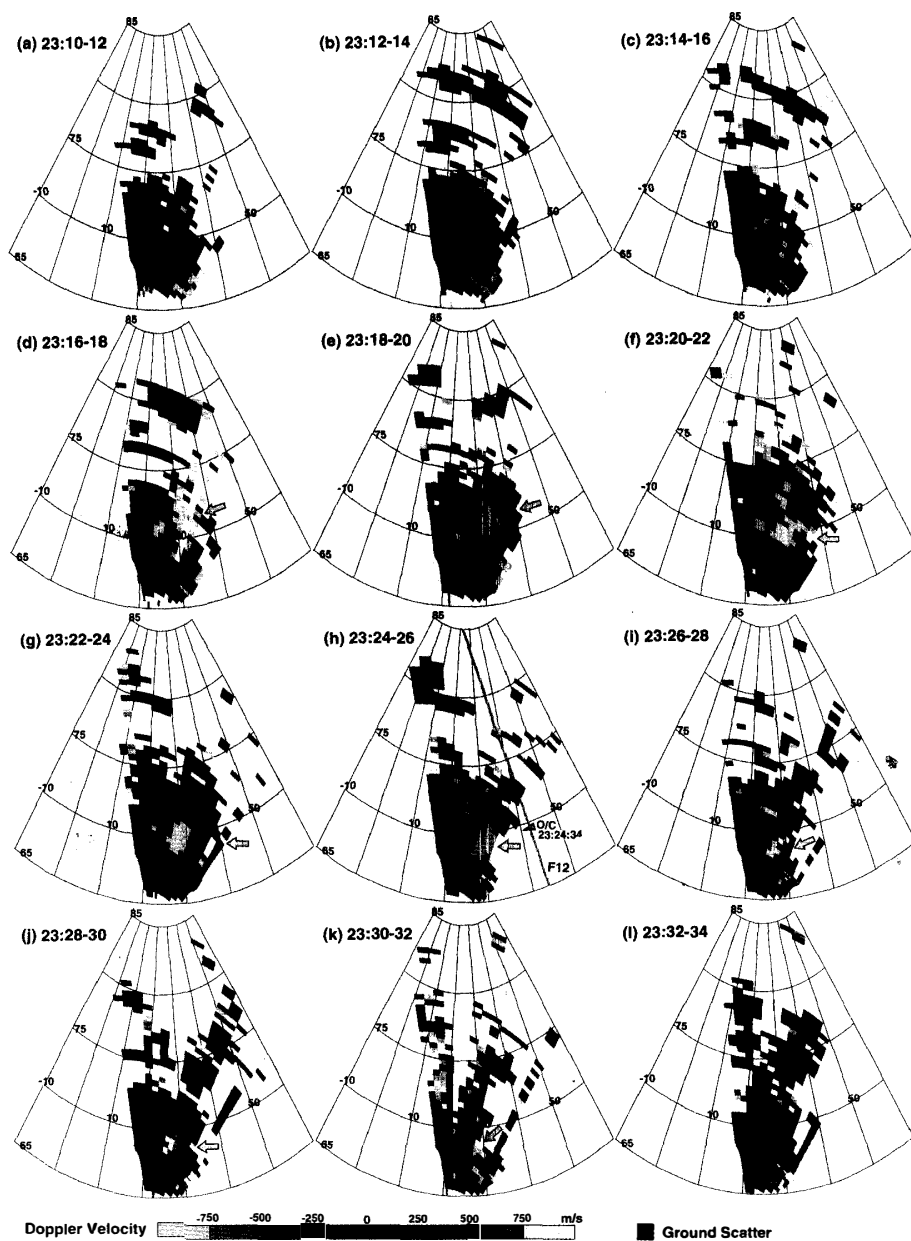


Fig. 2. At time sequence of line-of-sight Doppler velocities observed by the Goose Bay radar. Two-dimensional maps were obtained every two minutes. The bursty plasma flow, indicated by yellowish green arrows, emerged at ≈ 2316 (panel d) and started to degenerate at ≈ 2326 (at the onset of the substorm expansion phase, panel i), and finally faded out at ≈ 2332 (panel l). DMSF-F12 passed over the field-of-view during this interval and observed the polar cap or open/closed boundary at 2324:34 (69.5°N , 42.5°E in AACGM coordinates); the trajectory of the satellite is shown in panel h by an orange curve together with the open/closed (O/C) boundary observation by a blue triangle on the trajectory.

of plasma convection in the common volume of the two radars. The two-dimensional maps thus determined (not shown here) showed that velocity vectors in the bursty flow region in Fig. 2 were directed almost towards the Goose Bay radar site, which allows us to discuss the bursty flow characteristics using only the Goose Bay data. Therefore, in this paper we have exclusively explored line-of-sight velocities of the Goose Bay radar in detail.

During the time interval of the bursty flow, DMSP-F12 passed over the field-of-view of the Goose Bay radar. The satellite moved from equator to pole and observed the polar cap or open/closed boundary at 2324:34 UT (69.5°N, 42.5°E in AACGM coordinates). The trajectory of the satellite is shown in Fig. 2h by an orange curve; the blue triangle on the spacecraft trajectory shows the open/closed (O/C) boundary. We can conclude from Fig. 2h that the bursty flow occurred at the polar cap boundary, suggesting that the equatorward migration of the bursty flow region corresponds to the equatorward motion of the polar cap boundary during the late substorm growth phase just prior to the expansion phase onset. As quantitative analysis will be given in the following, the migration speed is several hundred m/s (<750 m/s) and the flow speed at the boundary is significantly higher than the migration speed. Therefore, it follows that in a frame moving with the separatrix (open/closed boundary surface),

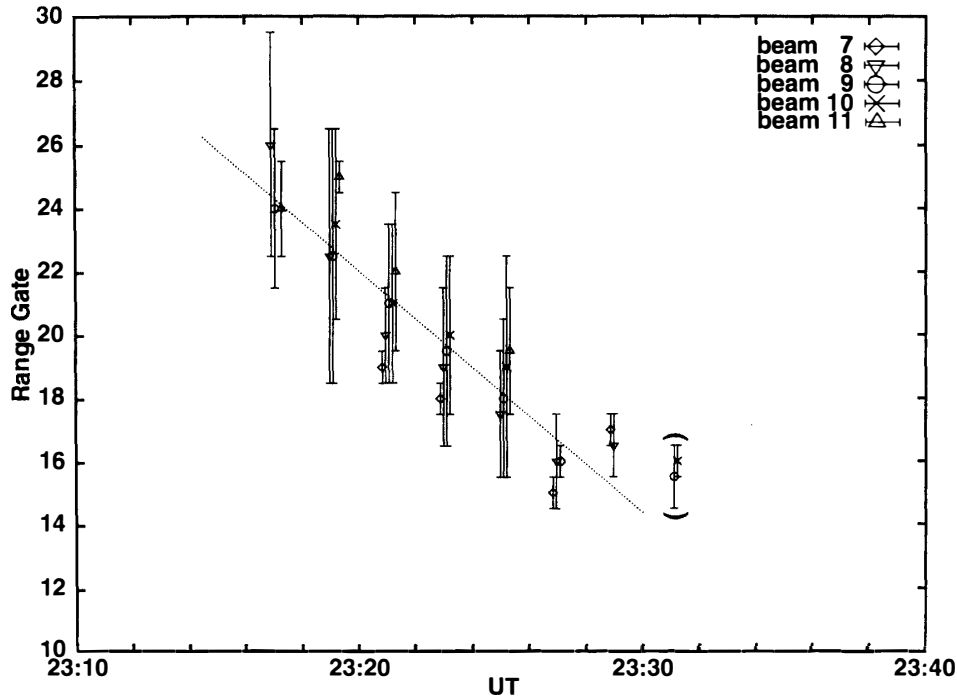


Fig. 3. The range gate extent of the "flow burst region" defined as a region of equatorward velocities greater than 750 m/s. Beam numbers are labeled from the westwardmost beam (beam 0) to the eastwardmost beam (beam 15) in order of number. The data in parentheses are excluded from the present analysis because of high error values in all beam-range bins. The oblique dotted line represents linear regression. The boundary motion speed determined from the linear regression is 575 ± 42 m/s.

there exists a plasma flow crossing the separatrix. In other words, a reconnection process exists at the boundary (*e.g.* DE LA BEAUJARDIÈRE *et al.*, 1991).

Figure 3 shows the range width of the “flow burst region”. Here we defined the flow burst region as a region with equatorward velocities greater than 750 m/s. Beam numbers are labeled from the westwardmost beam (beam 0) to the eastwardmost beam (beam 15) in order of number. For the last scan during the bursty flow interval (2330–32, Fig. 2k), error estimates of Doppler velocities for all the range-beam bins of the flow burst region were greater than 150 m/s. Since in this analysis we have employed a criterion of 150 m/s for a maximum error value for the data to be effective, in Fig. 3, the flow burst region in the last scan is put in parentheses. The oblique dotted line in Fig. 3 is a linear regression line of the boundary motion; the last-scan data in parentheses are not included in the regression. Here one range gate corresponds to 45 km. Therefore, from the linear regression, the speed of the boundary motion is estimated to be 575 ± 42 m/s. On the other hand, the mean flow speed of the flow burst region is shown in Fig. 4 together with its error and standard deviation. As we mentioned above, we have excluded the data with errors greater than 150 m/s in the statistics. The shaded bar represents the boundary motion speed determined from Fig. 3. The mean flow speed in each scan is significantly greater than the boundary motion speed; therefore, we can conclude that reconnection occurred during the bursty flow interval.

We can estimate the reconnection electric field using the formula $E_{\text{rec}} = B (V - U)$,

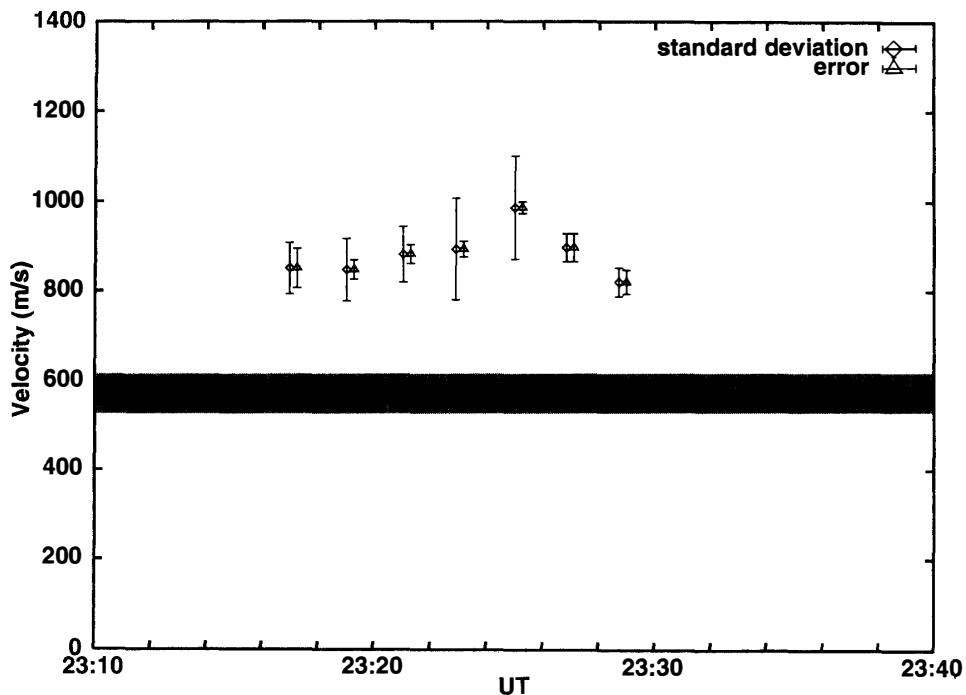


Fig. 4. The mean plasma flow speed of the flow burst region in each scan together with its standard deviation and error. The shaded bar shows the boundary motion speed determined from the linear regression in Fig. 3.

where V and U represent the speeds of the plasma flow and the boundary motion, respectively, and $B \approx 47000$ nT is the F -region magnetic field strength in the flow burst region. With $U=580$ m/s and $V=880$ m/s (total average) determined from Figs. 3 and 4, we obtain $E_{rec}=14$ mV/m. We can also estimate the reconnection voltage along the X line. If we assume that the average reconnection region is elongated from beam 7 to beam 11 and at range 20, then the azimuthal scale of the reconnection region is 290 km at 400 km altitude. With these values, the reconnection voltage is inferred to be 4.1 kV, which is very low as compared with the typical value observed in the dayside cusp.

We have also analyzed another event occurred on October 27, 1995. The morphology was exactly the same as the example demonstrated here. The bursty flow appeared during the late growth phase of a substorm and disappeared prior to the expansion phase onset. The boundary motion speed U was 670 m/s equatorward, whereas the mean flow speed V was 890 m/s equatorward. With the magnetic field strength $B \approx 48000$ nT in the flow burst region, the reconnection electric field is estimated to be 11 mV/m for this second case. As for the reconnection voltage, it is inferred to be 4.0 kV for an estimated longitudinal scale of 380 km.

Acknowledgments

We thank P. T. NEWELL and C.-I. MENG at Applied Physics Laboratory, the Johns Hopkins University, for processing DMSP particle data, which were originally provided by National Geophysical Data Center. We also thank E. FRIIS-CHRISTENSEN at Danish Meteorological Institute for providing Greenland magnetometer data, G. J. VAN BEEK at Geological Survey of Canada for providing Canadian magnetometer data, Canadian Space Agency (CSA) and T. HUGHES at CSA for providing CANOPUS (Canadian Auroral Network for the Open Program Unified Study) magnetometer data, and the Auroral Observatory, University of Tromsø, for providing Norwegian magnetometer data.

References

- BHAVNANI, K. H. and HEIN, C. A. (1994): An improved algorithm for computing altitude dependent corrected geomagnetic coordinates. Phillips Lab. Tech. Rep. No. PL-TR-94-2310, Phillips Lab., Hanscom Air Force Base, Mass.
- DE LA BEAUJARDIÈRE, O., LYONS, L. R. and FRIIS-CHRISTENSEN, E. (1991): Sondrestrom Radar measurements of the reconnection electric field. *J. Geophys. Res.*, **96**, 13907–13912.
- GREENWALD, R. A., BAKER, K. B., DUDENEY, J. R., PINNOCK, M., JONES, T. B. *et al.* (1995): DARN/SuperDARN: A global view of the dynamics of high-latitude convection. *Space Sci. Rev.*, **71**, 761–796.

(Received May 30, 1997; Revised manuscript accepted July 23, 1997)